



Published in final edited form as:

*J Biophotonics*. 2016 March ; 9(3): 208–212. doi:10.1002/jbio.201500181.

## Cuffing-based photoacoustic flowmetry in humans in the optical diffusive regime

Yong Zhou, Jinyang Liang, and Lihong V. Wang

Washington University in St. Louis, Department of Biomedical Engineering, Optical Imaging Laboratory, 1 Brookings Drive, Campus Box 1097, St. Louis, Missouri 63130

### Abstract

Measuring blood flow speed in the optical diffusive regime in humans has been a long standing challenge for photoacoustic tomography. In this work, we proposed a cuffing-based method to quantify blood flow speed in humans with a handheld photoacoustic probe. By cuffing and releasing the blood vessel, we can measure the blood flow speed downstream. In phantom experiments, we demonstrated that the minimum and maximum measurable flow speeds were 0.035 mm/s and 42 mm/s, respectively. In human experiments, flow speeds were measured in three different blood vessels: a radial artery in the right forearm, a radial artery in the index finger of the right hand, and a radial vein in the right forearm. Taking advantage of the handheld probe, our method can potentially be used to monitor blood flow speed in the clinic and at the bedside.

### Keywords

blood flow; optical diffusive regime; photoacoustic tomography; cuffing; in human

Blood flow mapping provides important information for the diagnosis and treatment of many diseases, such as stroke<sup>[1]</sup> and atherosclerosis<sup>[2]</sup>. Doppler ultrasound (US) is the most frequently used technique to measure blood flow in humans. However, because of the poor ultrasonic scattering contrast between blood and extravascular tissue, Doppler US cannot measure slow blood flow, which limits its use mainly to evaluating blood flow in the major arteries and veins<sup>[3]</sup>. Optical methods, such as Doppler optical coherence tomography<sup>[4]</sup> and laser speckle flowmetry<sup>[5]</sup>, cannot measure blood flow in humans in the optical diffusive regime due to the limited penetration of ballistic photons in biological tissue<sup>[6]</sup>.

With high blood detection contrast and deep penetration<sup>[6–10]</sup>, photoacoustic tomography (PAT) may provide a way to measure slow blood flow in the diffusive regime in humans. In PAT, short light pulses, usually from a laser, excite the target<sup>[7]</sup>. Following absorption of the light, an initial temperature rise induces a pressure rise due to the photoacoustic (PA) effect. The pressure rise then propagates as a PA wave and is finally detected by an ultrasonic transducer. Each laser pulse yielded a one-dimensional depth-resolved PA image (A-line) by recording the time course of PA signals. Because blood absorbs visible light much more strongly than most other tissue components, PAT can detect blood with high contrast. In

addition, by detecting ultrasonic signals, which have much lower scattering than optical signals in tissue, PAT can image deep with high spatial resolution. So far, PAT has detected blood vessels *in vivo* at 3.5 cm depth<sup>[11]</sup>.

Many PAT-based methods have been proposed to measure blood flow. In 2007, Fang et al. developed Doppler PA flowmetry to measure flowing particles<sup>[12]</sup>. Different from Doppler US, which detects scattering-based signals, Doppler PA detects absorption-based signals, and calculates the flow velocity based on their frequency shift. However, this method can measure only sparse particles, and it becomes less accurate when the detection axis is perpendicular to the flow direction. In 2009, the same group reported M-mode PA flowmetry<sup>[13]</sup>, which estimated the flow speed by quantifying the “slow-time” PA amplitude changes due to the moving particle. Note that the “slow-time” PA amplitude is defined as a series of maximum PA amplitudes from an A-line sequence. This method enabled measuring flow perpendicular to the detection axis. Based on similar ideas, time-domain PA auto-correlation<sup>[14]</sup> and frequency-domain PA Doppler bandwidth broadening<sup>[15]</sup> were proposed to measure blood flow in mice *in vivo*. To eliminate the measurement error resulting from the particle size, cross-correlation based PA flowmetry<sup>[16, 17]</sup> was introduced and also demonstrated in mice. For human imaging, however, because vessels are often more deeply embedded than they are in mice, PAT images these vessels with significantly degraded spatial resolutions<sup>[18, 19]</sup>. As the detection voxel size increases, there is a corresponding decrease in the slow-time PA signal changes due to the flowing particles or red blood cells<sup>[20]</sup>. When these changes are smaller than the other PA signal changes induced by, for example, thermal noise, it is difficult to extract flow information. In the end, none of existing methods has yet been applied to humans.

In this work, we present a cuffing-based method to measure blood flow speed in humans. Aided by a common sphygmomanometer, PAT successfully measured blood flow in humans for the first time. This procedure has three steps. First, a window along the blood vessel of interest is imaged. Second, the blood flow upstream of the window is stopped by cuffing the blood vessel with the sphygmomanometer. A high pressure (220 mg Hg in our experiments) is maintained in the cuff for a short time (e.g., 10 seconds) until there is almost no blood left in the vessel in the imaging window. Finally, the sphygmomanometer is quickly released, and the blood flow speed is calculated by monitoring the blood wash-in process.

To test our method, we employed a commercialized linear-array-transducer based PAT system<sup>[21, 22]</sup> (Vevo LAZR, VisualSonics, Toronto, ON, Canada), as shown in Fig. 1(a–b). A Nd:YAG laser combined with an optical parameter oscillator provided tunable illumination wavelengths from 680 nm to 970 nm. To achieve deep penetration, 850 nm was chosen for our experiments. The laser pulse had a width around 10 ns and a repetition rate of 20 Hz. The light was coupled to an optical fiber bundle that was divided into two rectangular fiber bundles (20 mm × 1.25 mm) with an illumination angle of 60° toward the tissue surface. The incident pulse fluence was around 5 mJ/cm<sup>2</sup>, below the safety limit set by the American National Standards Institute for this wavelength. A 256-element linear-array-transducer, with a central frequency of around 21 MHz (one-way bandwidth, 78%) and a size of 20 mm × 3 mm, detected ultrasonic signals. The array and the fiber bundles were aligned coaxially and confocally to maximize the system’s sensitivity. Because the data

acquisition system contained only 64 channels, a 4:1 electronic multiplexer was used to acquire ultrasonic signals from all the transducer elements. Thus, with a 20 Hz laser, the two-dimensional frame rate was reduced to 5 Hz to obtain a full-width image. However, the frame rate could be increased up to 20 Hz with fewer receiving channels and thus a smaller field of view (FOV). In our experiments, a frame rate of 10 Hz was used with a FOV of about  $12\text{ mm} \times 10\text{ mm}$ , along the axial and lateral directions of the array, respectively.

We first conducted phantom experiments to demonstrate the feasibility of our method for measuring blood flow speed in the diffusive regime. As shown in Fig. 1(c), to mimic a deeply embedded blood vessel, silastic tubing with an inner diameter of  $300\text{ }\mu\text{m}$  (11-189-15E, Fisher Scientific, Houston, TX) was overlaid by a piece of chicken breast tissue with a 2 mm thickness. Fresh bovine blood (910, QUAD FIVE INC., Ryegate, MT) was flowed inside the tubing at different speeds controlled by a syringe pump (BSP-99M, Braintree Scientific, Braintree, MA). As shown in Figs. 2(a)–(b), the blood wash-in process at different flow speeds could be accurately imaged. In those images, each column represents the one-dimensional PA amplitude image of the tubing in the FOV at a given time point. With increasing time, more blood flowed into the tubing in the imaging window. By quantifying how fast the blood front moved, the flow speed could be calculated, as shown in Fig. 2(c). As shown in Fig. 2(d), the measured flow speed agreed well with the preset values. The measured minimum flow speed was  $0.035\text{ mm/s}$ , which is smaller than the typical blood flow speed in capillaries in humans and also slower than the lowest flow speed that Doppler US can measure, i.e.,  $1\text{ mm/s}$ <sup>[3]</sup>. We also tested the maximum measurable flow speed. To measure the moving speed of the blood front, we have to at least image it twice. Thus, based on current frame rate (10 Hz) and FOV (10 mm along the tubing direction), in theory our maximum measurable flow speed should be around  $50\text{ mm/s}$ . However, as shown in Fig. 2(e), as the preset flow speed increased, the measurement error increased as well, which was probably due to the decreased number of times that the blood front was imaged. In our experiment, the maximum measured flow speed was around  $42\text{ mm/s}$ .

We then performed human experiments to show the capability of our method for measuring blood flow speed *in vivo*. As shown in Fig. 3, there were three different imaging sites in our human experiments — a radial artery in the right forearm, a radial artery in the index finger of the right hand, and a radial vein in the right forearm. As shown in Figs. 3(a) and (b), the upper arm was cuffed by the sphygmomanometer to measure the blood flow speed in the radial arteries in the forearm and finger. To measure venous flow speed, instead of cuffing, we directly compressed the radial vein close to the wrist and monitored a downstream location of the same vein, as shown in Fig. 3(c). All methods and experimental procedures were carried out in accordance with the guidelines of The Institutional Review Board of Washington University in St. Louis. All experimental protocols were approved by The Institutional Review Board of Washington University in St. Louis.

As shown in Figs. 4(a)–(c), the cuffing and releasing processes for all tested locations were clearly imaged. Before cuffing the vessel, both the top and bottom walls of the vessel could be detected. After cuffing, the blood vessel almost completely disappeared in the PA images. Once the cuff was released, the blood vessel appeared again. The recovery speed depended on the blood flow speed: For the big artery, the recovery process was the fastest;

while for the vein, the process was the slowest. The whole cuffing and releasing process in these three blood vessels can be observed in Videos 1 (forearm radial artery), 2 (index finger radial artery), and 3 (forearm radial vein). Based on the same procedure as in the phantom experiments, the flow speeds in these blood vessels were calculated to be around 44 mm/s (forearm radial artery), 20 mm/s (index finger radial artery), and 10 mm/s (forearm radial vein). The measured blood flow speeds were close to the flow speeds measured with US Doppler, which were 50 mm/s, 18 mm/s, and 9.3 mm/s, respectively. Based on the experimental results, we conclude that our cuffing-based PA method can measure blood flow in humans in both big and small blood vessels.

When the blood vessel is completely cuffed, there is almost no detectable blood in the downstream but blood accumulates under pressure upstream of the cuffing spot. Thus, the initial post-release blood wash-in process is a surge, which diminishes to normal flow with increased distance from the cuffing spot. In our measurements, we sought to avoid surge effects by setting the downstream imaging locations at ~ 5 cm for the vein flow measurement and more than 30 cm for arterial measurements.

In summary, for the first time to our knowledge, we measured blood flow speed in humans with PAT. By cuffing and releasing the targeted blood vessels, the flow information could be extracted. In phantom experiments, the minimum and maximum measurable flow speeds with the current system were experimentally quantified to be around 0.035 mm/s and 42 mm/s, respectively. We further applied our method to measure both arterial and venous flow speeds in humans. Because we used a handheld photoacoustic probe, our method can easily be used to detect blood flow speed both in the clinic and at home.

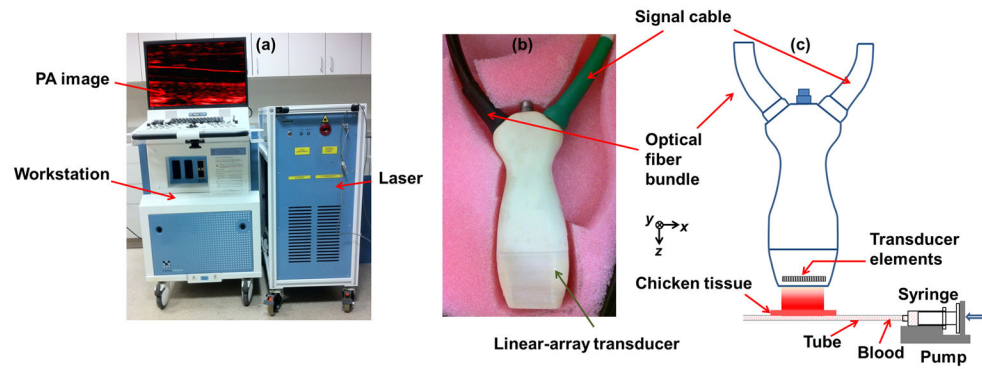
## Acknowledgments

The authors would like to thank Guo Li, Alejandro Garcia-Urbe, and Jun Ma for experimental assistance and helpful discussion, and Prof. James Ballard for manuscript editing. This work was sponsored in part by National Institutes of Health grants DP1 EB016986 (NIH Director's Pioneer Award), R01 CA186567 (NIH Director's Transformative Research Award), R01 EB016963, S10 RR026922, and R01 CA159959. L.W. has a financial interest in Microphotoacoustics, Inc. and Endra, Inc., which, however, did not support this work.

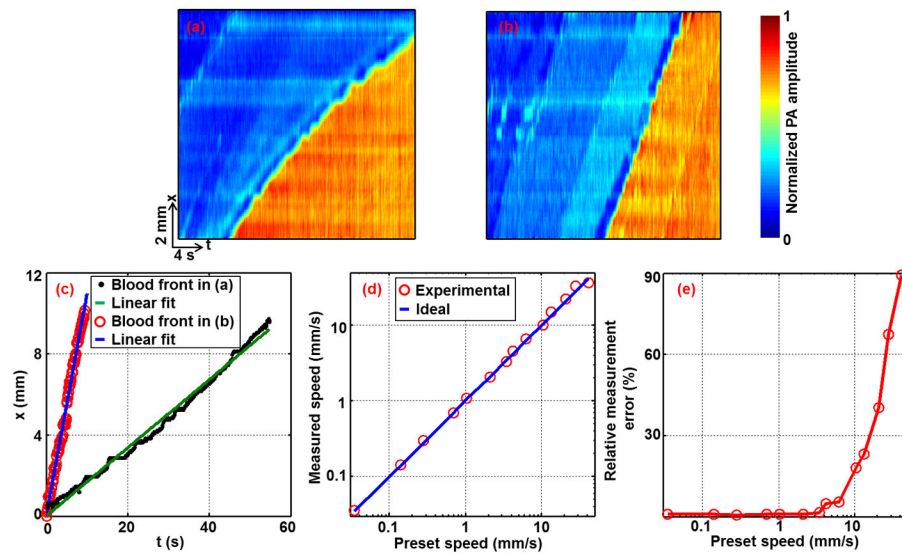
## References

1. Zhu XH, Chen JM, Tu TW, Chen W, Song SK. Simultaneous and noninvasive imaging of cerebral oxygen metabolic rate, blood flow and oxygen extraction fraction in stroke mice. *Neuroimage*. 2013; 64:437–447. [PubMed: 23000789]
2. Beraia M, Beraia G. Investigation of the Blood Flow at the Boundary Layer by the Magnetic Resonance Angiography in Atherosclerosis. *Atherosclerosis*. 2014; 235(2):E156–E156.
3. Tchacarski V. Atlas of diagnostic ultrasound. 2015
4. Zhao YH, Chen ZP, Saxer C, Xiang SH, de Boer JF, Nelson JS. Phase-resolved optical coherence tomography and optical Doppler tomography for imaging blood flow in human skin with fast scanning speed and high velocity sensitivity. *Opt Lett*. 2000; 25(2):114–116. [PubMed: 18059800]
5. Ayata C, Dunn AK, Gursoy-Ozdemir Y, Huang ZH, Boas DA, Moskowitz MA. Laser speckle flowmetry for the study of cerebrovascular physiology in normal and ischemic mouse cortex. *J Cerebr Blood F Met*. 2004; 24(7):744–755.
6. Wang LHV, Gao L. Photoacoustic Microscopy and Computed Tomography: From Bench to Bedside. *Annu Rev Biomed Eng*. 2014; 16:155–185. [PubMed: 24905877]

7. Wang LHV, Hu S. Photoacoustic Tomography: In Vivo Imaging from Organelles to Organs. *Science*. 2012; 335(6075):1458–1462. [PubMed: 22442475]
8. Beard P. Biomedical photoacoustic imaging. *Interface Focus*. 2011; 1(4):602–631. [PubMed: 22866233]
9. Zhou Y, Xing W, Maslov KI, Cornelius LA, Wang LV. Handheld photoacoustic microscopy to detect melanoma depth in vivo. *Opt Lett*. 2014; 39(16):4731–4734. [PubMed: 25121860]
10. Hai PF, Yao JJ, Maslov KI, Zhou Y, Wang LHV. Near-infrared optical-resolution photoacoustic microscopy. *Opt Lett*. 2014; 39(17):5192–5195. [PubMed: 25166107]
11. Kim C, Erpelding TN, Jankovic L, Pashley MD, Wang LHV. Deeply penetrating in vivo photoacoustic imaging using a clinical ultrasound array system. *Biomed Opt Express*. 2010; 1(1): 278–284. [PubMed: 21258465]
12. Fang H, Maslov K, Wang LV. Photoacoustic doppler effect from flowing small light-absorbing particles. *Phys Rev Lett*. 2007; 99(18)
13. Fang H, Wang LHV. M-mode photoacoustic particle flow imaging. *Opt Lett*. 2009; 34(5):671–673. [PubMed: 19252588]
14. Chen SL, Xie ZX, Carson PL, Wang XD, Guo LJ. In vivo flow speed measurement of capillaries by photoacoustic correlation spectroscopy. *Opt Lett*. 2011; 36(20):4017–4019. [PubMed: 22002371]
15. Yao JJ, Maslov KI, Shi YF, Taber LA, Wang LHV. In vivo photoacoustic imaging of transverse blood flow by using Doppler broadening of bandwidth. *Opt Lett*. 2010; 35(9):1419–1421. [PubMed: 20436589]
16. Zhou Y, Liang JY, Maslov KI, Wang LHV. Calibration-free in vivo transverse blood flowmetry based on cross correlation of slow time profiles from photoacoustic microscopy. *Opt Lett*. 2013; 38(19):3882–3885. [PubMed: 24081077]
17. Liang JY, Zhou Y, Maslov KI, Wang LHV. Cross-correlation-based transverse flow measurements using optical resolution photoacoustic microscopy with a digital micromirror device. *J Biomed Opt*. 2013; 18(9)
18. Wang, LV.; Wu, H. *Biomedical Optics: Principles and Imaging*. WILEY; 2007.
19. Yao J, Wang LV. Sensitivity of photoacoustic microscopy. *Photoacoustics*. 2014; 2(2):87–101. [PubMed: 25302158]
20. Zhou Y, Yao J, Maslov KI, Wang LV. Calibration-free absolute quantification of particle concentration by statistical analyses of photoacoustic signals in vivo. *J Biomed Opt*. 2014; 19(3): 37001. [PubMed: 24589987]
21. Needles A, Heinmiller A, Sun J, Theodoropoulos C, Bates D, Hirson D, Yin M, Foster FS. Development and Initial Application of a Fully Integrated Photoacoustic Micro-Ultrasound System. *Ieee T Ultrason Ferr*. 2013; 60(5):888–897.
22. Zhou Y, Li G, Zhu L, Li C, Cornelius LA, Wang LV. Handheld photoacoustic probe to detect both melanoma depth and volume at high speed in vivo. *J Biophotonics*. 2015; 1(7)



**Fig. 1.** Photographs of the PAT system (a) and the linear-array-transducer (b). The workstation has a 64-channel data acquisition system, a data processing system, and an image display interface. (c) A schematic of the array in the phantom experiments.

**Fig. 2.**

Phantom experiments. PA signal amplitude versus lateral position  $x$  and time  $t$  measured at different preset flow speeds: (a) 0.14 mm/s and (b) 1.1 mm/s. (c) Time course of the blood fronts in (a) and (b), where the slope of each linear fit directly represents the flow speed. (d) Log-log plot of the measured flow speeds versus the preset values. (e) Semi-log plot of the relative errors of the measured speeds in (d).



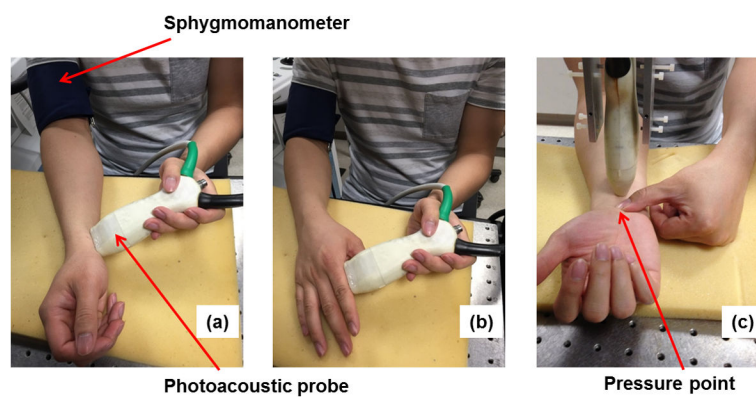


**Fig. 3.** Photographs of the human experiments with imaging sites at a forearm radial artery (a), an index finger radial artery (b), and a forearm radial vein (c).



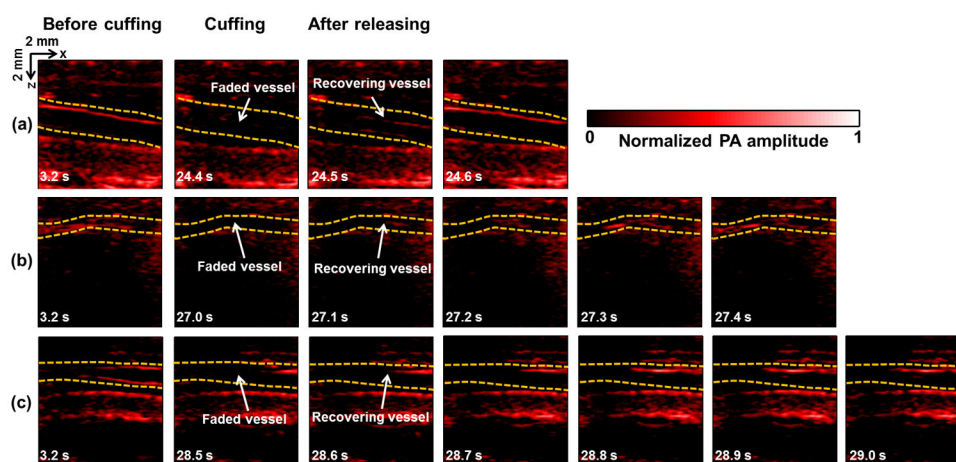


**Fig. 4.** Human experiments. Representative PA images of a forearm radial artery (a), an index finger radial artery (b), and a forearm radial vein (c) before cuffing, during cuffing, and after releasing. The yellow dashed lines indicate the blood vessel regions.